The Spectroscopic Consequences of C−H···π H-Bonding: $C_6H_6-(C_4H_2)_n$ Clusters with $n = 1$ and 2

Christopher Ramos,[†] Paul R. Winter,[‡] Jaime A. Stearns, and Timothy S. Zwier*

Department of Chemistry, Purdue University, 560 Oval Drive, West Lafayette, Indiana 47907-2084

Received: July 28, 2003; In Final Form: September 30, 2003

The ultraviolet and infrared spectra of the $C_6H_6-(C_4H_2)_n$ complexes with $n = 1$ and 2 have been formed and studied in a supersonic expansion using resonant two-photon ionization (R2PI), resonant ion-dip infrared spectroscopy (RIDIRS), and IR−UV hole-burning spectroscopy. A T-shaped structure is deduced for the complex, with the C_4H_2 centered, end on, over the benzene ring. This C−H···π H-bond shifts the frequency of the vibronic transitions of C_6H_6 by 161 cm^{-1} to the blue. The acetylenic CH stretch fundamental of C_4H_2 is localized and split by formation of the π H-bond. The H-bonded CH stretch fundamental is lowered in frequency by about 40 cm^{-1}, increased in intensity by more than a factor of 2, and split by a Fermi resonance that is turned on by the complexation. The $C_6H_6-(C_4H_2)_2$ complex has a structure that makes the S_1-S_0 origin transition weakly allowed and possesses an infrared spectrum that has acetylenic CH stretch absorptions due to free CH, aromatic π-bound CH, and a more weakly π-bound CH. Its structure is tentatively assigned as a cyclic, "pinwheel" structure.

I. Introduction

This article describes the infrared and ultraviolet spectroscopy of the $C_6H_6-C_4H_2$ complex, formed and studied in a supersonic expansion. There are several motivations for this work. First, C_4H_2-containing clusters bear some relevance for the cold atmosphere of Titan (~70 K), one of the moons of Saturn. One of the intriguing, unsolved mysteries of Titan's atmosphere is the molecular source of the visible absorbing haze that enshrouds the moon.[1,2] Larger conjugated hydrocarbons formed from the photochemical reactions of diacetylene are one likely possibility, motivating recent studies of the photochemical reactions of C_4H_2 with various hydrocarbons known to be present in Titan's atmosphere.[3−10] The photochemical reactions of diacetylene occur out of long-lived triplet states following efficient intersystem crossing from the singlet vibronic levels accessed by ultraviolet photoexcitation.[11] Such studies have recently identified the aromatic benzene as a dominant primary product in the reaction of C_4H_2* with 1,3-butadiene,[7] and phenylacetylene ($C_6H_5C_2H$) and phenyldiacetylene ($C_6H_5C_4H$) as the dominant primary products in the reaction of C_4H_2* with benzene:[9]

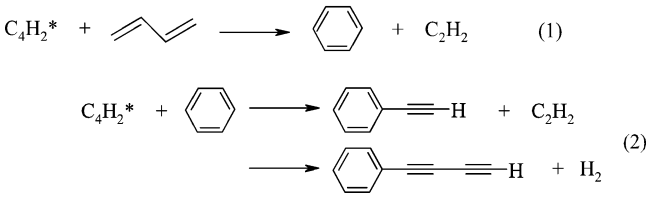

Such aromatics are likely candidates for detection by the Huygens probe, which will investigate Titan's atmosphere in unprecedented detail and with much greater sensitivity than remote observations have allowed to date.[12] While many of the reactions leading to the visible-absorbing haze are gas phase, it also is likely that photochemistry in aerosols may play an important role. The photochemistry of gas-phase clusters can serve as models for the aerosol reactions.

Second, structural characterization of the $C_6H_6-C_4H_2$ complex reported herein can serve as a foundation for future studies of the complex's "half-collision" reaction dynamics.[13−18] The bimolecular reaction between C_4H_2* and benzene can be compared with analogous photochemistry initiated within the $C_6H_6-C_4H_2$ complex, in which the reaction is initiated out of the well-defined starting geometry determined by the complex, removing averaging over approach geometries inherent to full-collision studies. The study of photochemical reactions in complexes is typically complicated by uncertainties about the starting composition or structure of the complex, since spectroscopic characterization can be hindered by the reaction itself. However, in the $C_6H_6-C_4H_2$ complex, both molecules are UV chromophores. One anticipates that the S_1-state of benzene will be photochemically unreactive toward C_4H_2. As a result, structural characterization of the $C_6H_6-C_4H_2$ complex can be carried out using the S_0-S_1 transition of C_6H_6 as a probe, employing resonant two-photon ionization (R2PI) and resonant ion-dip infrared (RIDIR) spectroscopies.[19,20] The ultraviolet absorptions that form reactive C_4H_2*$-C_6H_6$ could then be probed and identified using UV−UV hole-burning methods with an unreactive C_6H_6*$-C_4H_2$ absorption as probe transition, followed by studies of the photochemical products so formed once the wavelengths of the C_4H_2*$-C_6H_6$ absorptions are known.

The present report provides the spectroscopic foundation for such photochemical studies. The combined infrared and ultraviolet data lead to a firm assignment of the complex to a C_{6v} symmetry structure in which C_4H_2 lies on the sixfold axis of benzene, with one of its CH groups pointing toward the ring, forming a CH hydrogen bond with the π cloud of benzene.

* To whom correspondence should be addressed. E-mail: zwier@purdue.edu.

[†] Present address: Department of Chemistry, Johns Hopkins University, Baltimore, MD 21218.

[‡] Present address: Chemir Analytical Services, 2672 Metro Blvd., Maryland Heights, MO 63043.

10.1021/jp036204u CCC: $25.00
Published on Web 11/08/2003

This structure for the complex, then, provides its own motivation for this work. There has been long-standing interest in the notion that CH groups can form weak hydrogen bonds with electronegative accepting groups, typically oxygen or nitrogen.[21,22] Among the types of CH hydrogen bonds noted in such studies are C−H···π hydrogen bonds involving aromatic acceptors. This doubly unconventional hydrogen bond has structural support from the analysis of X-ray crystallographic databases[21,22] but lacks a corresponding spectroscopic foundation. The unusual polarity of the acetylenic CH bond makes it capable of forming some of the strongest CH hydrogen bonds, and C≡C−H···X hydrogen bonds do possess CH stretch fundamentals that are both shifted to lower frequency and increased in intensity, as is common for traditional XH···Y hydrogen bonds.[23] By spectroscopically characterizing the $C_6H_6-C_4H_2$ complex, both in the ultraviolet and infrared, we are afforded a clear view of the spectroscopic consequences of C−H···π hydrogen bonding in the isolated complex.

Finally, the $C_6H_6-(C_4H_2)_n$ clusters are close analogues of the $C_6H_6-(C_2H_2)_n$ clusters that have been studied previously in the ultraviolet.[24,25] Comparison of the two suggests a close similarity between their structures.

II. Experimental Section

The experimental apparatus used for these experiments has been described in detail elsewhere.[4,8] The following is a brief description. Gas samples of diacetylene were synthesized in our laboratory following the method of Armitage[26] which is described in detail by Ramos.[27] Pure C_4H_2 was collected and diluted to a 5−7% mixture in helium and stored in a 3 L gas tank or lecture bottle. For studies of the $C_6H_6-(C_4H_2)_n$ clusters, gas-phase benzene/C_4H_2/He mixtures were made up in a gas manifold and used immediately. Typical gas mixtures of 1−6% benzene and 3% diacetylene in helium at a total pressure of 2 bar were used. Both C_6H_6 and C_6D_6-containing clusters were studied. Complexes were formed in the supersonic expansion produced by a pulsed valve (Jordan, 800 μm diameter) operating at 10 Hz. Resonant two-photon ionization spectroscopy is carried out using time-of-flight mass analysis. One-color, resonant two-photon ionization of the clusters is accomplished using either the S_0-S_1 transition of benzene or the S_0-S_2 transition of C_4H_2 in the complex. The frequency-doubled output of a Nd:YAG pumped, tunable dye laser (ScanMate IIe, Lambda Physik) is used for this purpose. Typical pulse energies of 0.1−0.5 mJ/pulse are used either unfocused or weakly focused with a 50-cm lens placed 30 cm from the ion source region.

Size-selected infrared spectra of $C_6H_6-(C_4H_2)_n$ clusters are recorded using resonant ion-dip infrared spectroscopy.[28] The ground-state population of a given cluster is monitored by fixing the wavelength of the ultraviolet laser to the vibronic transition of interest in the R2PI spectrum and gating on the ion signal due to the cluster size of interest. An infrared beam, produced by a Nd:YAG-pumped infrared parametric converter (LaserVision), is spatially overlapped with the UV beam in the ion source region of the TOFMS and precedes the UV pulse by about 200 ns. When the infrared wavelength is resonant with an infrared transition due to the cluster whose ion signal is being monitored, infrared absorption will remove population from the ground state, producing a depletion in the neutral ground-state population that is reflected in a decrease in the ion signal produced by the UV source. Operation of the IR source at 5 Hz and the UV source at 10 Hz allows data to be collected in active baseline subtraction mode. This mode records the difference in ion signal between successive UV laser shots, one without and one with the IR present. This differential ion signal is averaged in the boxcar integrator and recorded by a data acquisition computer.

III. Calculations

Possible structures for the $C_6H_6-C_4H_2$ and $C_6H_6-(C_4H_2)_2$ complexes were tested by carrying out full geometry optimizations using Gaussian98[29] for a range of starting geometries chosen to explore various types of cluster structures. Density functional theory (DFT) calculations using the Becke3LYP functional[30] and a 6-31+G* basis set[31] were used as initial calculations that explored the various possible stable structures in an efficient manner. The recent extensive calculations of the closely analogous $C_6H_6-C_2H_2$ complex by Tsuzuki et al.[23] show that DFT calculations do not provide a quantitatively accurate description of the intermolecular binding in cases such as this, where dispersive interactions contribute substantially to the total binding energy. As a result, the DFT calculations were followed by MP2 calculations using the correlation-consistent polarized double-ζ (cc-pVDZ) basis set developed by Dunning and coworkers[32,33] to obtain optimized structures, energies, and, for the 1:1 complexes, harmonic vibrational frequencies and zero-point energy (ZPE) corrections. Computational limitations precluded calculation of MP2 frequencies for the 1:2 clusters, so DFT results were used. Binding energies for the complexes were corrected for basis set superposition error (BSSE) using the counterpoise method.[34] Proper scaling of the MP2 harmonic frequencies for Fermi resonance analysis was accomplished by performing the same level of calculation on acetylene and diacetylene and scaling those frequencies to match experimental data. This procedure resulted in a scale factor of 0.953 for acetylenic CH stretches, while all other types of vibrations were left unscaled. The DFT frequencies reported for the 1:2 complex were scaled by 0.957, chosen so the calculated free C−H stretch in the 1:1 complex matched experimental data.

IV. Results and Structural Analysis

A. R2PI Spectroscopy. Figure 1a and 1b present overview R2PI spectra of the region near the origin and 6^1_0 S_0-S_1 transitions of benzene, monitoring the $[C_6H_6-C_4H_2]^+$ and $[C_6H_6]^+$ mass channels, respectively. The most intense transition in Figure 1a is assigned to the 6^1_0 transition of the $C_6H_6-C_4H_2$ complex, occurring 161 cm^{-1} above the corresponding 6^1_0 transition of C_6H_6 monomer (Figure 1b), which is the dominant, vibronically allowed transition in C_6H_6 in this region. The corresponding 6^1_0 transition of the $C_6D_6-C_4H_2$ complex is shifted another 181 cm^{-1} to the blue, an amount nearly identical to the 180 cm^{-1} shift of the 6^1_0 transition of C_6D_6 monomer relative to C_6H_6 monomer (38611 cm^{-1}).[35] This indicates that complexation of C_4H_2 to benzene produces little differential zero-point energy shift upon electronic excitation.

The electronic frequency shift of benzene's 6^1_0 transition induced by C_4H_2 (+161 cm^{-1}) is notable both for its magnitude and sign. As summarized in Table 1, numerous past studies of C_6H_6···X complexes have noted that molecules that hydrogen bond to benzene's π cloud (e.g., HCl, H_2O, CH_3OH, $HCCl_3$) produce a blueshift in benzene's S_0-S_1 transition, while those that interact with benzene via dispersive interactions (e.g., benzene, CCl_4) typically produce a redshift.[19] By such a measure, C_4H_2 appears to be forming a hydrogen bond with benzene. Furthermore, the frequency shift is substantially larger than that of many good hydrogen-bond donors, including all

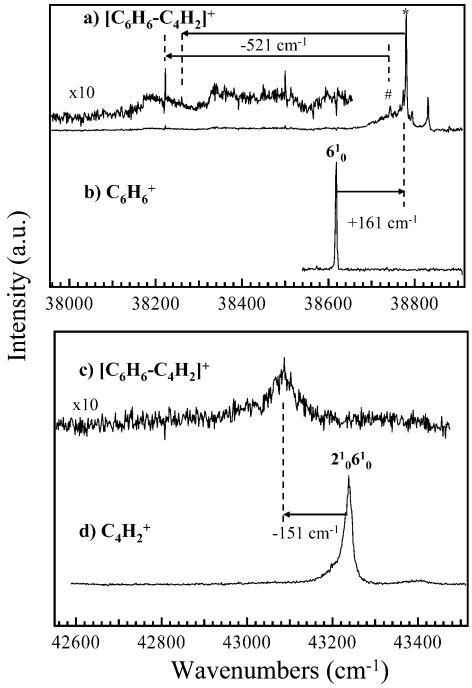

Figure 1. One-color resonant two-photon ionization spectra monitoring the (a, c) $(C_6H_6-C_4H_2)^+$, (b) $C_6H_6^+$, and (d) $C_4H_2^+$ mass channels, respectively. The scans of the complex used the room-temperature vapor pressure of benzene and a 3% C_4H_2 in helium gas mixture at a backing pressure of 2 bar, expanded through an 800-μm nozzle. (a, b) The 6^1_0 transition of the $C_6H_6-C_4H_2$ complex, marked with an asterisk, is shifted $+161$ cm^{-1} relative to the corresponding transition in the C_6H_6 monomer. The transition tentatively assigned as the 6^1_0 transition of $C_6H_6-(C_4H_2)_2$ is marked with a #, appearing in this mass channel by fragmentation following photoionization. The anticipated positions of the 0^0_0 transitions of the 1:1 and 1:2 complexes are shown in (a), 521 cm^{-1} below the 6^1_0 bands. (c, d) The $2^1_0 6^1_0$ S_0-S_2 transition of the $C_6H_6-C_4H_2$ complex is shifted -151 cm^{-1} from the corresponding transition in the C_4H_2 monomer.

TABLE 1: Electronic Frequency Shifts of $C_6H_6-X_n$ Complexes with $n = 1, 2$

		electronic shift (cm^{-1})	
	X	$n = 1$	$n = 2$
H-bond donors	HCl	+125	
	$CHCl_3$	+178	
	H_2O	+49	+75
	CH_3OH	+41	+80
	C_2H_2	+136	+116/+125
	C_4H_2	+161	+124
nonpolar	C_6H_6	−41	
	CCl_4	−68	

those listed in the table except $CHCl_3$. It is also somewhat greater than that observed in $C_6H_6-C_2H_2$, with its $+136$ cm^{-1} shift.[24]

Surrounding the 6^1_0 transition of the $C_6H_6-C_4H_2$ complex are a broad background ion signal that peaks near the 6^1_0 band of the complex and a short Franck−Condon progression involving a 50 cm^{-1} intermolecular vibration. IR−UV hole-burning scans (Section IV.C) confirmed that the peaks in this progession are indeed from the same ground state as the main 6^1_0 transition and thus also belong to the $C_6H_6-C_4H_2$ complex.

The other transitions arise from fragmentation of larger $(C_6H_6)_n-(C_4H_2)_m$ clusters following photoionization, a common occurrence in $C_6H_6-X_n$ clusters in which π H-bonds are involved.[19] In particular, the band at 38744 cm^{-1} is tentatively assigned to the $C_6H_6-(C_4H_2)_2$ cluster. This band also appears very weakly in the $[C_6H_6-C_4H_2]^+$ mass channel and is present in $[C_6H_6-C_4H_2]^+$ because of loss of a single C_4H_2 molecule from the cluster following photoionization. The transitions assigned to the $C_6H_6-(C_4H_2)_2$ cluster (hereafter the 1:2 cluster) are strikingly similar to the corresponding bands in $C_6H_6-(C_2H_2)_2$,[24] which also appear in the 1:1 mass channel slightly redshifted from the bands due to the 1:1 complex. Further evidence for the assignment will come from the infrared spectroscopy and IR−UV hole-burning spectroscopy (Section IV.B, C).

The overview R2PI scan of Figure 1a also encompasses the S_0-S_1 origin region. Because the $X(^1A_{1g})-A(^1B_{2u})$ transition of benzene monomer is dipole-forbidden, it gains intensity by vibronic coupling to the strongly allowed E_{1u} state of benzene via vibrations of e_{2g} symmetry. ν_6 is an e_{2g} vibration, and the 6^1_0 band forms a false origin 521 cm^{-1} above the dipole-forbidden 0^0_0 transition at 38 090 cm^{-1}. Symmetry arguments show that complexation of a molecule X will produce a weakly allowed origin transition if the sixfold symmetry of benzene is reduced to lower than threefold symmetric in the C_6H_6-X complex.[36] Arguments of this type have been used in the past to constrain the geometries of several benzene-containing complexes.[19] In all cases studied to date, the ν_6 excited-state frequency (521 cm^{-1}) is unchanged by complexation, because the complexed molecule typically sits in an out-of-plane position where it does not perturb the ν_6 vibration, an in-plane deformation of the aromatic ring. An arrow in Figure 1a indicates the expected position of the origin transition of the $C_6H_6-C_4H_2$ complex, 521 cm^{-1} below the observed 6^1_0 transition. No origin transition is observed, with an upper limit on the origin intensity of 1% of the 6^1_0 transition. On this basis alone, one can surmise that the C_4H_2 molecule sits on the sixfold axis of benzene.[19] Two possible orientations of C_4H_2 are possible, either (i) forming a T-shaped complex in which C_4H_2 sits on the sixfold axis with one of its CH groups pointing in toward the ring, or (ii) taking up an off-axis orientation (e.g., lying down on one face of the aromatic ring), but undergoing internal rotation relative to benzene to produce a *vibrationally averaged* structure which is still sixfold symmetric. Note that a weak origin transition is observed in the $C_6H_6-C_4H_2^+$ mass channel at 38 223 cm^{-1} (Figure 1a). This transition is 521 cm^{-1} below the transition at 38 744 cm^{-1}, which we have already tentatively assigned to the 1:2 cluster.

Figure 1c and 1d present one-color R2PI scans in the $2^1_0 6^1_0$ region of the S_0-S_2 transition of C_4H_2, monitoring the $C_6H_6-C_4H_2^+$ and $C_4H_2^+$ mass channels, respectively. This electronic transition in C_4H_2 ($^1\Sigma_g^+-{}^1\Delta_u$) is dipole-forbidden in $D_{\infty h}$ but gains intensity through vibronic coupling with the $^1\Pi_u$ state via π_g vibrations, of which ν_6 is the most prominent.[37−39] The vibronic structure of C_4H_2 is dominated by a long progression in ν_2, the symmetric C≡C stretch, built off of the 6^1_0 transition. The intense band in the $C_4H_2^+$ mass channel is the $2^1_0 6^1_0$ transition of the C_4H_2 monomer, which has been used in previous photochemical studies of C_4H_2 to initiate bimolecular photochemistry. This transition is inherently broad (∼18 cm^{-1} fwhm), even under expansion cooling, consistent with its fast intersystem crossing to the triplet manifold. With benzene in the expansion, a weak, broad transition is observed in the $[C_6H_6-C_4H_2]^+$ mass channel, shifted 151 cm^{-1} down in wavenumber position from the monomer transition. This transition is tentatively assigned to the $C_6H_6-C_4H_2$ complex.

B. RIDIR Spectroscopy. Figure 2b presents a resonant ion-dip infrared scan of the $C_6H_6-C_4H_2$ complex over the CH stretch region, taken while monitoring the 6^1_0 transition of $C_6H_6-C_4H_2$ marked by an asterisk in Figure 1a. The corre-

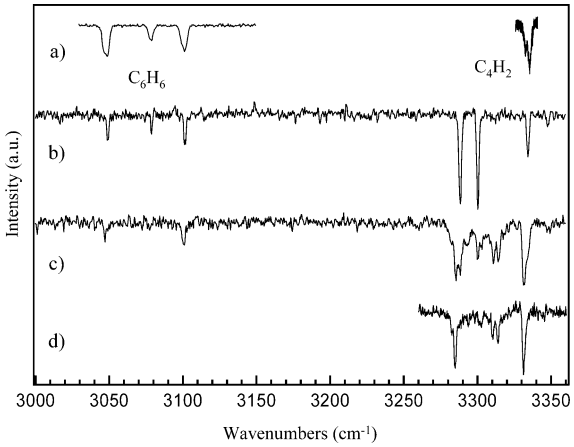

Figure 2. Resonant ion-dip infrared spectra of the C_6H_6 monomer (left-hand side of trace a) and C_4H_2 monomer (right-hand side of trace a) in the CH stretch region. (b) and (c): Corresponding RIDIR spectra of the $C_6H_6-C_4H_2$ and $C_6H_6-(C_4H_2)_2$ complexes, monitoring the ion signal with the R2PI laser fixed on the bands marked with an * and #, respectively, in Figure 1. (d) RIDIR scan of the $C_6D_6-(C_4H_2)_2$ complex.

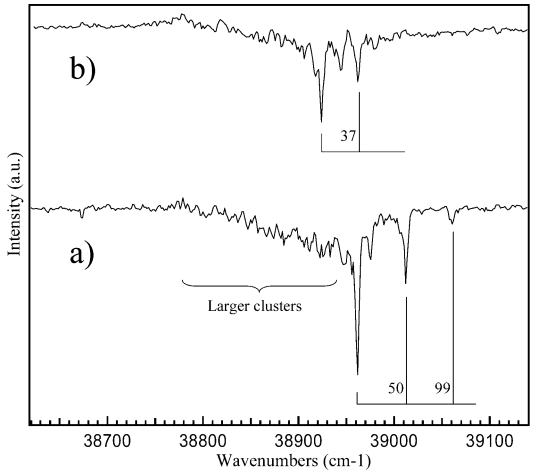

Figure 3. IR−UV hole-burning scans with the infrared hole-burn laser fixed at (a) 3300 and (b) 3310 cm^{-1}, corresponding to infrared transitions due to $C_6D_6-C_4H_2$ and $C_6D_6-(C_4H_2)_2$, respectively. The tail on the low-frequency side of the scans is due to larger $(C_6D_6)_n-C_4H_2$ and $(C_6D_6)_n-(C_4H_2)_2$ clusters fragmenting into the $1:1^+$ mass channel following photoionization.

sponding scans of the C_6H_6 monomer and C_4H_2 monomer taken while monitoring the C_6H_6 6^1_0 transition and the C_4H_2 $2^1_0 6^1_0$ transitions are shown in Figure 2a for comparison. The three transitions observed in the aromatic CH stretch region of the benzene monomer have been thoroughly studied and are a Fermi resonance triad involving the single dipole-allowed CH stretch fundamental coupling to two combination bands involving CH bending vibrations.[28] These bands retain their frequencies and relative intensities in the $C_6H_6-C_4H_2$ complex, indicating that complexation with C_4H_2 has little effect on the anharmonic coupling that produces this pattern of bands.

The acetylenic CH stretch region of the C_4H_2 molecule undergoes much more dramatic changes upon complexation to benzene. The C_4H_2 monomer possesses a single IR-allowed antisymmetric CH stretch fundamental (Figure 2a) with a center frequency of 3333 cm^{-1}.[40] The P- and R-branches anticipated of a parallel band of linear C_4H_2 are clearly observed. The symmetric CH stretch of C_4H_2 is known from Raman studies to be nearly coincident with the antisymmetric stretch, with the two bands split by less than one wavenumber.[40]

Surprisingly, in the $C_6H_6-C_4H_2$ complex, the acetylenic CH stretch region is composed of not one, but three bands, appearing at 3288, 3300, and 3334 cm^{-1}. A fourth weak band at 3347 is also observed at higher IR laser powers, just above the noise level. The 3334 cm^{-1} band is nearly coincident with the band in C_4H_2 monomer and is thereby assigned as a "free" acetylenic CH stretch. The two main bands are shifted by −46 and −34 cm^{-1} from the free C_4H_2 stretch and are much more intense than the band at 3334 cm^{-1}. In traditional XH···Y hydrogen bonds, both the frequency shift and the intensity increase are clear signatures of hydrogen bonding.[41] The presence of these shifted bands, then, is indicative of formation of a CH···π hydrogen bond with one of the CH groups. Because of the weak coupling between the two CH bonds in C_4H_2, frequency shifts of this magnitude must be associated with localization of the two CH stretch fundamentals on the two CH groups of C_4H_2. The fact that there are two bands in the π H-bonded C−H stretch region (3288 and 3300 cm^{-1}) suggests a Fermi resonance splitting of the π H-bonded CH stretch fundamental. We will return to this point in the discussion section.

A RIDIR scan taken while monitoring the band at 38744 cm^{-1}, tentatively assigned to the $C_6H_6-(C_4H_2)_2$ cluster and marked with a # in Figure 1a, is shown in Figure 2c. The RIDIR spectrum of the corresponding band assigned to $C_6D_6-(C_4H_2)_2$ is shown just below it for comparison. A complication of both of these spectra is that the ion signal at this UV wavelength contains a contribution from a broad background because of higher *n*:*m* clusters, appearing in this mass channel because of fragmentation following photoionization. We were never able to remove this background entirely. As a result, the RIDIR scans in Figure 2c contain a small contribution from this background. A RIDIR scan taken while monitoring this background (at 38956 cm^{-1}, not shown) shows only weak, broad depletions and gains, consistent with the background arising from higher clusters. If this background changes little with ultraviolet wavelength, then the sharp bands observed in Figure 2c are due to the sharp transition in the R2PI scan.

The acetylenic CH stretch region of the 1:2 cluster contains a complex set of bands reminiscent of the $C_6H_6-C_4H_2$ complex above it. The band at 3334 cm^{-1} is assigned to the free acetylenic CH stretch, while the complicated set of bands in the 3285−3315 cm^{-1} region must involve some CH···π interaction either with benzene or another C_4H_2 molecule. The bands in this region appear as doublets, with splittings of about 3 cm^{-1}. The presence of this wealth of bands may arise either from changes in the Fermi resonance mixing present in $C_6H_6-C_4H_2$, or from the existence of unique environments for the four CH bonds of the two C_4H_2 molecules in the cluster. Both the level of complexity and the closely spaced doublets are less evident in the $C_6D_6-(C_4H_2)_2$ spectrum shown in Figure 2d. The Fermi triad characteristic of benzene is also observed weakly in the 3000−3100 cm^{-1} region of $C_6H_6-(C_4H_2)_2$.

C. IR−UV Hole-Burning Scans. Figure 3a and 3b presents IR−UV hole-burning scans with the IR hole-burning frequency chosen to be resonant with a unique IR transition due to $C_6D_6-C_4H_2$ (3300 cm^{-1}) and $C_6D_6-(C_4H_2)_2$ (3310 cm^{-1}), respectively. The hole-burn scan identifies all UV transitions that share an infrared absorption at these wavenumber positions. The spectrum in Figure 3a confirms the earlier statement that the bands at 38 962, 39 012, and 39 061 cm^{-1} are all due to the $C_6D_6-C_4H_2$ complex, forming a Franck−Condon progression with 50 cm^{-1} spacing.

The 6^1_0 transition of the 1:2 complex is shifted −38 cm^{-1} from the 6^1_0 transition of the 1:1 complex. This is closely analogous to the spectroscopy of the $C_6H_6-(C_2H_2)_n$ clusters,

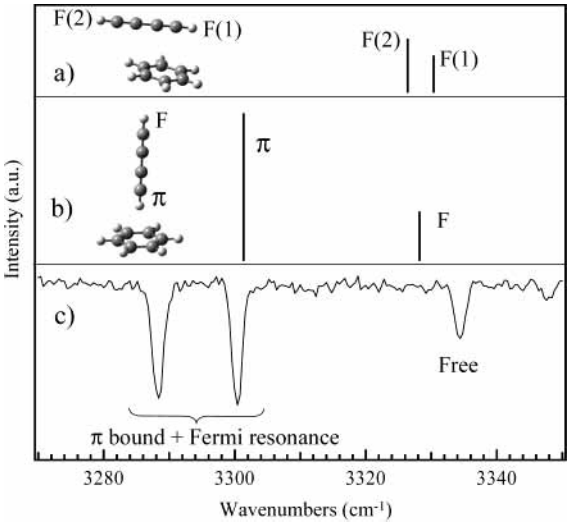

Figure 4. (a, b) Calculated harmonic vibrational frequencies and infrared intensities of the acetylenic CH stretch modes of the (a) flat and (b) upright structures of the $C_6H_6-C_4H_2$ complex. The calculated structures, computed at the MP2/cc-pVDZ level of theory, are shown as insets. The vibrational frequency calculations were carried out at the MP2/cc-pVDZ level of theory. Vibrational frequencies are scaled by 0.953. (c) Experimental RIDIR spectrum for comparison.

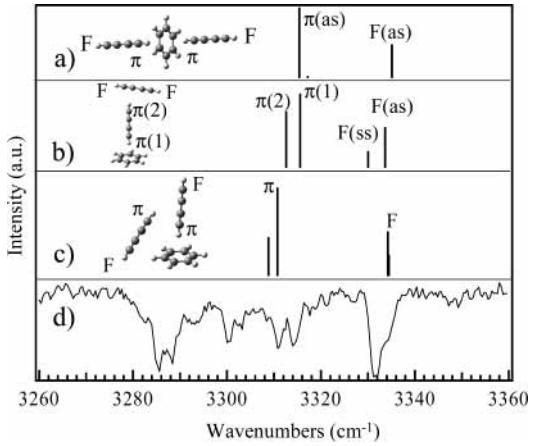

Figure 5. (a−c) Calculated harmonic vibrational frequencies and infrared intensities of the acetylenic CH stretch modes of the pictured structures of the $C_6H_6-(C_4H_2)_2$ complex. The vibrational frequency calculations were carried out at the B3LYP/ 6-31+G* level of theory and scaled by 0.957. (d) Experimental RIDIR spectrum of $C_6H_6-(C_4H_2)_2$.

where the 6^1_0 transition of the 1:1 complex is shifted from the benzene monomer transition by +136 cm^{-1}, while those due to the two 1:2 isomers are shifted back to lower frequency by −10 and −21 cm^{-1} from the $n = 1$ transition.[24] The spectrum in Figure 3b is very similar in appearance to that of the 1:1 complex above it, sharing a short Franck−Condon progression in a 37 cm^{-1} mode, whose first member appears as a shoulder on the 6^1_0 band of the $n = 1$ complex. In principle, IR−UV hole burning could also confirm whether the band at 38 223 cm^{-1} is indeed due to the 1:2 cluster. However, its small size prevented such a determination.

Both hole-burning scans also possess a broad background tailing off to the low-frequency side of the corresponding 6^1_0 transitions. This background is reduced in intensity relative to the sharp bands as the benzene concentration is lowered. We thus tentatively assign these low-frequency tails to $(C_6D_6)_n-C_4H_2$ and $(C_6D_6)_n-(C_4H_2)_2$ clusters, respectively.

D. Ab Initio Calculations. Computations at the MP2/cc-pVDZ level of theory indicate the lowest energy configuration for the benzene−diacetylene complex is that shown in Figure 4b, in which the diacetylene molecule is on end, centered on the benzene ring. The other bound structure identified for the 1:1 complex, shown in Figure 4a, has the diacetylene molecule lying flat on benzene in a π stacked configuration. The ZPE- and BSSE-corrected binding energies for the structures in Figure 4a and b are 0.85 and 2.06 kcal/mol, respectively.

Three structures were considered for the 1:2 complex, all of which incorporate a second diacetylene molecule to the most stable 1:1 complex. Structure I, shown in Figure 5a, adds the second C_4H_2 to the opposite side of the benzene ring to form a "doubly upright" structure, retaining the sixfold symmetry of benzene. Structure II (Figure 5b) also possesses a vibrationally averaged sixfold axis once internal rotation of the diacetylene at the top of the "T" is considered. This structure combines the lowest energy structures for the $C_6H_6-C_4H_2$ ("upright") and $C_4H_2-C_4H_2$ (T-shaped) complexes. The computed total binding energy for this structure is approximately the sum of that for the two dimers. Structure III (Figure 5c) is a cyclic or pinwheel structure, in which the second C_4H_2 accepts a hydrogen bond from the benzene CH groups, and is stabilized by a weak interaction with the upright C_4H_2. It is the analogue of the benzene or naphthalene trimer structure,[42] in which two aromatic subunits have been replaced by diacetylene. The sixfold symmetry of benzene is lost in this structure. Binding energies, corrected for BSSE, were nearly identical for Structures I and III, while Structure II was about 1.1 kcal/mol less strongly bound. Results of these calculations are summarized in Table 2.

TABLE 2: Calculated Binding Energies for the $C_6H_6-C_4H_2$ and $C_6H_6-(C_4H_2)_2$ Clusters with Basis Set Superposition Error Correction (BSSE) and Zero-Point Energy Correction (ZPE)[a,b]

		ΔE	BSSE	ZPE	ΔE (corrected)
1:1	upright	4.34	−1.71	−0.57	2.06
	flat	2.76	−1.81	−0.10	0.85
1:2	I	8.38	−3.33		5.05
	II	6.30	−2.41		3.89
	III	8.43	−3.40		5.03

[a] All calculations carried out at the MP2/cc-pVDZ level of theory. [b] All energies in kcal/mol.

V. Discussion

A. The C−H···π H-Bond in the $C_6H_6-C_4H_2$ Complex. The combined results of the R2PI and RIDIR scans lead to a firm assignment for the structure of the $C_6H_6-C_4H_2$ complex. The lack of an S_0-S_1 origin transition points to a structure that retains the sixfold symmetry of benzene. The electronic frequency shift to the blue by the complex is consistent with C_4H_2 donating a H-bond to benzene's π cloud. The infrared spectrum shows a "free CH" and a π H-bonded CH stretch (which is Fermi resonance split), with the latter fundamental both lower in frequency and increased in intensity. This is consistent with the calculated harmonic frequencies and infrared intensities for the upright structure, which correctly predict both the frequency lowering and intensity increase observed experimentally (Figure 4). The structure with the diacetylene molecule lying flat on the ring (Figure 4a) is inconsistent with experiment, since neither CH stretch is significantly redshifted from the free position. We therefore assign the observed transitions to a $C_6H_6-C_4H_2$ structure in which diacetylene stands upright on the sixfold axis of benzene, acting as a hydrogen bond donor in a C−H···π H-bond. This, too, is consistent with the predictions of calcula-

tion, which find the upright structure (Figure 4b) to be the most stable structure for the complex (Table 2).

Given that the complex contains a CH···π H-bond, it is worthwhile to comment on its characteristics by comparison to other, more conventional H-bonds. The calculations predict a binding energy for this doubly unconventional CH···π H-bond of about 720 cm^{-1}. The observation of the $C_6H_6-C_4H_2$ 6^1_0 transition in the parent mass channel is a probable indicator that the experimental binding energy in the S_1 state is more than 521 cm^{-1}. This places a lower bound on the ground-state binding energy of $D_0 = 521 + 161\ cm^{-1} = 682\ cm^{-1}$. A binding energy of of this magnitude is somewhat smaller than a typical XH···Y hydrogen bond (e.g., D_0(HF dimer) = 1062 cm^{-1}).[43] However, it is comparable to that found for the $C_6H_6-H_2O$ complex (810 cm^{-1})[44] and is significantly greater than the purely dispersive interaction present in the p-difluorobenzene-Ar complex (337 cm^{-1}).[45]

In our previous discussion, we have assumed that the natural direction of shift of the CH stretch fundamental in response to H-bond formation would be to shift to lower frequency, as the XH stretch fundamental does in a conventional XH···Y hydrogen bond. However, there are many examples of CH···Y hydrogen bonds that blueshift rather than redshift.[46] Recent theoretical effort has sought to establish a physical basis for the unusual blueshift. A unified model has been put forward by Hermansson whereby the leading prerequisite for a blueshift upon hydrogen bond formation is the sign of the dipole derivative for the donor CH bond. A positive dipole derivative produces a redshift, while a negative derivative has the potential to produce a blueshift. It appears that the π bound diacetylenic CH group has the "typical" positive dipole derivative, in which the dipole moment is increased as the bond is stretched.

B. The Fermi Resonance Splitting of the π H-Bonded CH Stretch Fundamental. We have not yet addressed the nature of the Fermi resonance that splits the π H-bonded CH stretch fundamental of C_4H_2 in the $C_6H_6-C_4H_2$ complex. This Fermi resonance is intriguing because it is not present either in the C_4H_2 monomer or on the free CH stretch of the complex. It would appear then that the formation of the C−H π H-bond brings this CH stretch fundamental into Fermi resonance with the state responsible for mixing. To assign the Fermi resonant state, it is helpful to recall that the σ_u CH stretch fundamental of acetylene monomer is split by a Fermi resonance with the $\nu_2 + \nu_4 + \nu_5$ combination band, forming a doublet at 3281.0 and 3294.9 cm^{-1}.[47] The ν_2, ν_4, and ν_5 normal modes of acetylene are the CC triple bond stretch (1974 cm^{-1}), the π_g CH bend (612 cm^{-1}), and the π_u CH bend (730 cm^{-1}), respectively.

Diacetylene monomer, meanwhile, exhibits no Fermi resonance in this region, with only a single σ_u CH stretch fundamental observed at 3334 cm^{-1} (Figure 2a). Three combination bands possess the correct symmetry to mix with the CH stretch fundamental (Table 3). However, those built off the lower frequency C≡C stretch are too low in energy to mix with the CH stretch, while the combination involving the higher frequency C≡C stretch is too high.

Fermi resonance is present at the hydrogen bound CH stretch in the $C_6H_6-C_4H_2$ complex but not at the free CH stretch. This behavior can be understood by examining the calculated frequencies, using acetylene and diacetylene as tests of the accuracy of the calculated vibrational frequencies (Table 3). The CH π hydrogen bond in the complex decouples the CH groups of the C_4H_2 molecule, giving a localized hydrogen bound CH stretch about 30 cm^{-1} to the red of the free CH, and a hydrogen bound CH bend shifted 66 cm^{-1} to the red of the free CH bend.

TABLE 3: Fermi Resonance Analysis for Acetylene, Diacetylene, and the $C_6H_6-C_4H_2$ Complex[a]

	calc combination band	CH stretch	
	C≡C str + 2 CH bend = total	calcd	expt
C_2H_2	1965 + 560 + 750 = 3275	3292	3281, 3295[b]
C_4H_2	2186 + 611 + 597 = 3394	3324	3329[b]
	1998 + 611 + 611 = 3220		
	1998 + 597 + 597 = 3192		
$C_6H_6{\cdot}C_4H_2$	2182 + 594 + 594 = 3370	3328	3334[c]
free CH	1995 + 594 + 594 = 3183		
$C_6H_6{\cdot}C_4H_2$	2182 + 660 + 660 = 3502	3301	3288, 3300[c]
bound CH	1995 + 660 + 660 = 3315		

[a] Frequencies calculated using MP2/cc-pVDZ, unscaled except for the CH stretch, which was scaled 0.953. [b] http://webbook.nist.gov.[47] [c] Present work.

So while the free CH behaves like diacetylene and shows no Fermi resonance, the frequency shifts due to hydrogen bonding bring the bound CH stretch into resonance with the combination band of the antisymmetric C≡C stretch (1995 cm^{-1}) plus two quanta of bound CH bend.

C. The R2PI Spectrum through the C_4H_2 Chromophore: Foundation for Photochemical Studies. So far, the discussion of the $C_6H_6-C_4H_2$ complex has been primarily based on the spectroscopy that used the benzene molecule as the electronic chromophore. However, it is worth commenting briefly on the R2PI spectrum in Figure 1c, which involves electronic excitation of the C_4H_2 molecule in the complex. First, it is this region of the spectrum where one anticipates the possibility that C_4H_2* + benzene "half-collison" reaction could occur.[9] However, the fact that the R2PI spectrum was recorded while monitoring the $[C_6H_6-C_4H_2]^+$ mass channel seems to indicate that reaction, if it occurs, takes place on a time scale that is long compared to absorption of a second photon to ionize the complex (i.e., within the 8-ns laser pulse). It is possible that the structure for the complex, in which C_4H_2 resides on the sixfold axis of benzene, discriminates against reaction, which involves attack of C_4H_2* at a benzene C−H bond. However, the identification of absorption features due to the complex is an important first step in pump−probe experiments designed to detect the product molecules phenylacetylene (C_8H_6) and phenyldiacetylene ($C_{10}H_6$).[9]

Second, the shift of the transition due to the $C_6H_6-C_4H_2$ complex when C_4H_2 is electronically excited (−151 cm^{-1}, Figure 1c) is equal in magnitude and opposite in sign to the shift that occurs when C_6H_6 is excited (+161 cm^{-1}, Figure 1a). This indicates that electronic excitation of C_4H_2 increases the strength of the π H-bond with benzene by 151 cm^{-1}, while electronic excitation of C_6H_6 decreases this bond by a similar amount.

D. The $C_6H_6-(C_4H_2)_2$ Complex. The spectroscopic characteristics of the $C_6H_6-(C_4H_2)_2$ complex are summarized below, including the deductions that can be drawn on their basis regarding its structure. As we shall see, the balance of spectroscopic evidence favors a cyclic or pinwheel structure for the $C_6H_6-(C_4H_2)_2$ cluster, like that shown in Figure 5c, though this assignment is less firm than that for $C_6H_6-C_4H_2$.

(1) The R2PI transitions assigned to the 1:2 cluster appear only in the $[1:1]^+$ mass channel. The efficient loss of a single C_4H_2 molecule from the cluster occurs following photoionization, much as occurs in many other $C_6H_6-(solvent)_n$ clusters.[19] This indicates that a large geometry change accompanies photoionization, which produces Franck−Condon factors to the ion that favor large internal energy in the cluster, leading to fragmentation. We surmise that the neutral 1:2 cluster retains a π H-bonded interaction with one or more C_4H_2 molecules, which

becomes unfavorable when the benzene becomes positively charged upon photoionization.

(2) The electronic frequency shift of the 1:2 cluster from the C_6H_6 monomer transition ($+124$ cm^{-1}) is also consistent with retention of a π H-bonded interaction. However, this shift is 37 cm^{-1} less than that in the 1:1 complex, suggesting that the second C_4H_2 binds in an inequivalent position relative to the first C_4H_2. The alternative structure, in which the second C_4H_2 molecule takes up an identical position to the first C_4H_2 on the opposite side of the benzene ring, would be anticipated to have an electronic frequency shift roughly twice that of the 1:1 complex. Furthermore, the redshift relative to the 1:1 complex is consistent with the C_4H_2 molecule accepting a hydrogen bond from benzene, rather than donating a hydrogen bond to the benzene π cloud.

(3) The presence of the origin transition at 38223 cm^{-1} in the R2PI spectrum is consistent only with a structure in which the sixfold axis of benzene is reduced to less than threefold symmetric. Of the three structures in Figure 5, only the pinwheel structure (Figure 5c) breaks the sixfold symmetry of benzene. In structure II, the second C_4H_2 molecule is spatially far removed from the benzene and would be anticipated to undergo nearly free internal rotation relative to benzene, creating a *vibrationally averaged* structure that retains the sixfold symmetry.

(4) The RIDIR spectrum of the 1:2 complex is qualitatively consistent with the pinwheel structure, possessing transitions in the acetylenic CH stretch region assignable to free CH stretch (3334 cm^{-1}), a Fermi diad due to a π H-bonded CH (3288 and 3300 cm^{-1}), and additional bands between these two extremes tentatively assigned to the diacetylene−diacetylene π H-bond in the pinwheel structure. The free acetylenic CH stretch region is broader and more intense in the 1:2 than in the 1:1 complex, consistent with the presence of two free CH groups. The redshifted Fermi diad appears at frequencies almost identical to those found in the 1:1 complex.

(5) The pinwheel structure (Figure 5c) is calculated to be significantly more strongly bound than the structure II (Figure 5b), and nearly identical in binding to the doubly upright structure I (Figure 5a).

(6) Finally, a comparison of the calculated vibrational frequencies and infrared spectra provide some support for the pinwheel structure but are also qualitatively consistent with the T-shaped isomer. Because of the size and floppiness of the minima for $C_6H_6-(C_4H_2)_2$ complex, the stick spectra of Figure 5 were generated at the B3LYP/6-31+G* level of theory. As a result, they are not quantitatively accurate and characteristically underestimate the magnitudes of the vibrational frequency shifts from the free CH stretch position. Nevertheless, the pinwheel structure has a set of two free C−H stretches, and two redshifted π H-bonded CH stretches. The vibrational frequency of this $C_4H_2-C_4H_2$ π-bound CH stretch should be quite sensitive to the orientation of the donor C_4H_2, such as structure II (where it is T-shaped) versus structure III (where it is at an oblique angle). If these angles are changed as the level of theory is increased, it will likely lead to better agreement between experiment and theory. Furthermore, we do not have an explanation for the additional splitting of bands in the π H-bonded CH stretch region. As a result, the assignment of the 1:2 cluster to the pinwheel structure must be considered tentative.

VI. Conclusions

The $C_6H_6-C_4H_2$ complex provides a clear example of a doubly unconventional C−H$\cdots\pi$ H-bond, in which C_4H_2 acts as a H-bond donor to benzene's π cloud, residing on the sixfold axis of benzene. The acetylenic CH group has an unusually high polarity for a CH bond, and this manifests itself both in the choice of structure for the complex, and in the spectroscopic consequences of hydrogen bond formation. The C−H$\cdots\pi$ H-bond localizes the CH stretch modes on the π-bound and free CH group and shifts the acetylenic CH stretch fundamental down in frequency by about -40 cm^{-1} relative to the free CH stretch. This is a frequency shift comparable in magnitude to that of the OH stretch of methanol induced by formation of the $CH_3OH\cdots\pi$ H-bond in the $C_6H_6-CH_3OH$ complex (-42 cm^{-1}). At the same time, the electronic frequency shift induced in benzene's S_0-S_1 transition by complexation with C_4H_2 is larger than any other H-bonding solvent so far studied, with the exception of $HCCl_3$. On the basis of this spectroscopic foundation, future studies which determine the binding energy or the photochemical reactivity of this complex seem warranted.

Acknowledgment. The authors gratefully acknowledge support from the NASA planetary atmospheres program (NAG5-12098). J.A.S. thanks NASA for a Graduate Student Research Fellowship.

References and Notes

(1) Strobel, D. F. *Icarus* **1974**, *21*, 446.
(2) Strobel, D. F. *Planet. Space Sci.* **1982**, *30*, 839.
(3) Bandy, R. E.; Lakshminarayan, C.; Frost, R. K.; Zwier, T. S. *Science* **1992**, *258*, 1630.
(4) Bandy, R. E.; Lakshminarayan, C.; Frost, R. K.; Zwier, T. S. *J. Chem. Phys.* **1993**, *98*, 5362.
(5) Frost, R. K.; Zavarin, G.; Zwier, T. S. *J. Phys. Chem.* **1995**, *99*, 9408.
(6) Frost, R. K.; Arrington, C. A.; Ramos, C.; Zwier, T. S. *J. Am. Chem. Soc.* **1996**, *118*, 4451.
(7) Arrington, C. A.; Ramos, C.; Robinson, A. D.; Zwier, T. S. *J. Phys. Chem. A* **1998**, *102*, 3315.
(8) Arrington, C. A.; Ramos, C.; Robinson, A. D.; Zwier, T. S. *J. Phys. Chem. A* **1999**, *103*, 1294.
(9) Robinson, A. G.; Winter, P. R.; Ramos, C.; Zwier, T. S. *J. Phys. Chem. A* **2000**, *104*, 10312.
(10) Robinson, A. G.; Winter, P. R.; Zwier, T. S. *J. Phys. Chem. A* **2002**, *106*, 4789.
(11) Glicker, S.; Okabe, H. *J. Phys. Chem.* **1987**, *91*, 437.
(12) Raulin, F.; Accaoui, B.; Razaghi, A.; Dang-Nhu, M.; Coustenis, A.; Gautier, D. *Spectrochim. Acta* **1990**, *46A*, 671.
(13) Keller, A.; Lawruszczuk, R.; Soep, B.; Visticot, J. P. *J. Chem. Phys.* **1996**, *105*, 4556.
(14) Briant, M.; Gaveau, M. A.; Fournier, P. R.; Mestdagh, J. M.; Visticot, J. P.; Soep, B. *Faraday Discuss.* **2001**, *118*, 209.
(15) Breckenridge, W. H. *J. Phys. Chem.* **1996**, *100*, 14840.
(16) McCoy, A. B.; Naaman, R. *Int. Rev.Phys. Chem.* **1999**, *18*, 459.
(17) Wittig, C.; Sharpe, S.; Beaudet, R. A. *Acc. Chem. Res.* **1988**, *21*, 341.
(18) Wheeler, M. D.; Anderson, D. T.; Lester, M. I. *Int. Rev. Phys. Chem.* **2000**, *19*, 501.
(19) Zwier, T. S. *Annu. Rev. Phys. Chem.* **1996**, *47*, 205.
(20) Zwier, T. S. *J. Phys. Chem. A* **2001**, *105*, 8827.
(21) Jeffrey, G. A.; Saenger, W. *Hydrogen Bonding in Biological Structures*; Springer-Verlag: New York, 1991.
(22) Jeffrey, G. A. *J. Mol. Struct.* **1999**, *485−486*, 293.
(23) Tsuzuki, S.; Honda, K.; Uchimaru, T.; Mikami, M.; Tanabe, K. *J. Am. Chem. Soc.* **2000**, *122*, 3746.
(24) Shelley, M. Y.; Dai, H.-L.; Troxler, T. *J. Chem. Phys.* **1999**, *110*, 9081.
(25) Carrasquillo, E.; Zwier, T. S.; Levy, D. H. *J. Chem. Phys.* **1985**, *83*, 4990.
(26) Armitage, J. B.; Jones, E. R. H.; Whiting, M. C. *J. Chem. Soc.* **1952**, 2014.
(27) Ramos, C. Ph.D. Thesis, Purdue University, 2002.
(28) Page, R. H.; Shen, Y. R.; Lee, Y. T. *J. Chem. Phys.* **1988**, *88*, 5362.
(29) Frisch, M. J.; Tucks, G. W.; Schlegel, H. B.; Scuseria, G. E.; Robb, M. A.; Cheeseman, J. R.; Zakrzewski, V. G.; J. A. Montgomery, Jr.; Stratmann, R. E.; Burant, J. C.; Dapprich, S.; Millam, J. M.; Daniels, A. D.; Kudin, K. N.; Strain, M. C.; Farkas, O.; Tomasi, J.; Barone, V.; Cossi, M.; Cammi, R.; Mennucci, B.; Pomelli, C.; Adamo, C.; Clifford, S.; Ochterski, J.; Petersson, G. A.; Ayala, P. Y.; Cui, Q.; Morokuma, K.; Malick,

D. K.; Rabuck, A. D.; Raghavachari, K.; Foresman, J. B.; Cioslowski, J.; Ortiz, J. V.; Baboul, A. G.; Stefanov, B. B.; G. Liu, A. L.; Liashenko, A.; Piskorz, P.; Komaromi, I.; Gomperts, R.; Martin, R. L.; Fox, D. J.; Keith, T.; Al-Laham, M. A.; Peng, C. Y.; Nanayakkara, A.; Challacombe, M.; Challacombe, M.; Gill, P. M. W.; Johnson, B.; Chen, W.; Wong, M. W.; Andres, J. L.; Gonzalez, C.; Head-Gordon, M.; Replogle, E. S.; Pople, J. A. *Gaussian 98*, Revision A.11.3; Gaussian, Inc.: Pittsburgh, PA, 1998.

(30) Becke, A. D. *J. Chem. Phys.* **1993**, *98*, 5648.

(31) Frisch, M. J.; Pople, J. A.; Binkley, J. S. *J. Chem. Phys.* **1984**, *80*, 3265.

(32) Woon, D. E.; Dunning, T. H., Jr. *J. Chem. Phys.* **1993**, *98*, 1358.

(33) Dunning, T. H. *J. Chem. Phys.* **1989**, *90*, 1007.

(34) Boys, S. F.; Bernardi, F. *Mol. Phys.* **1970**, *19*, 553.

(35) Weber, T.; von Bargen, A.; Riedle, E.; Neusser, H. J. *J. Phys. Chem.* **1990**, *92*, 90.

(36) Gotch, A. J.; Garrett, A. W.; Zwier, T. S. *J. Phys. Chem.* **1991**, *95*, 9699.

(37) Bandy, R. E.; Lakshminarayan, C.; Zwier, T. S. *J. Phys. Chem.* **1992**, *96*, 5337.

(38) Lamotte, J.; Binet, C.; Romanet, R. *J. Chim. Phys.* **1977**, *74*, 577.

(39) Chang, K. W.; Graham, W. R. M. *J. Mol. Spectrosc.* **1982**, *94*, 69.

(40) Owen, N. L.; Smith, C. H.; Williams, G. A. *J. Mol. Struct.* **1987**, *161*, 33.

(41) Pimentel, G. C.; McClellan, A. L. *The Hydrogen Bond* W. H. Freeman: San Francisco, CA, 1960.

(42) Benharash, P.; Gleason, M. J.; Felker, P. M. *J. Phys. Chem. A* **1999**, *103*, 1442.

(43) Miller, R. E. *Acc. Chem. Res.* **1990**, *23*, 10.

(44) Courty, A.; Mons, M.; Dimicoli, N.; Piuzzi, F.; Gaigeot, M. P.; Brenner, V.; Depujo, P.; Millie, P. *J. Phys. Chem. A* **1998**, *102*, 6590.

(45) Bellm, S. M.; Moulds, R. J.; Lawrance, W. D. *J. Chem. Phys.* **2001**, *115*, 10709.

(46) Hermansson, K. *J. Phys. Chem. A* **2002**, *106*, 4695.

(47) http://webbook.nist.gov.